

# Study of martensite transformation and microstructural evolution of Cu–Al–Ni–Fe shape memory alloys

## Effect of heat treatments

Koksal Yildiz · Mediha Kok

Received: 30 July 2013 / Accepted: 3 September 2013 / Published online: 9 October 2013  
© Akadémiai Kiadó, Budapest, Hungary 2013

**Abstract** In this study, variations in the transformation temperature, crystal structure, and microstructure of the arc melted alloy having nominal composition of Cu–13%Al–4%Ni–4%Fe (in mass%) were investigated for two different treatment conditions, homogenized and heat treated at 950 °C for 1 h. For both conditions, transformation temperature of the alloy was examined by DSC and it was determined as ~200 °C, similar to the value for Cu–Al–Ni alloys given in the literature. The crystal structure of the martensite Cu–13%Al–4%Ni–4%Fe (in mass%) alloy was identified as 18R using XRD. By heat treatment performed at 950 °C, diffraction peaks become more distinct. The microstructure of the alloy was studied with the help of optical microscope as a result of which parallel martensite plates and precipitates were detected. Microhardness value of the alloy was found as 361 and 375 Hv for homogenized and heat-treated conditions, respectively.

**Keywords** Cu–Al–Ni–Fe alloy · Martensite transformation · Heat treatment · Differential scanning calorimetry · Microhardness

## Introduction

Shape memory alloys are considered as an important system of alloys as these functional materials are used in sensor and actuator applications. In the last decade, they have experienced a remarkable technological development [1, 2]. Among different shape memory alloys, Cu-based alloys developed in 1960s have reasonable shape memory effect

and low cost making them remarkable commercial alloys for practical applications [3]. On the other hand, fundamental problems in their usage are based on their low thermal stability and insufficient mechanical strength. Cu-based alloys face with martensite stabilization problem as a result of which they lose their thermoelastic properties [4]. Among different Cu-based shape memory alloys, Cu–Al–Ni alloys are popular as they have wide range of transformation temperatures and small hysteresis [5]. With their serviceability to temperatures up to 200 °C and technological advantages, Cu–Al–Ni alloys have been developed as alternative materials to the classical Cu–Zn–Al and Ti–Ni alloys [6]. Shape memory effect of Cu–Al–Ni based alloys is very sensitive to the composition of each element and specific compositions, generally those with 11–14.5 % Al and 3–5 % Ni, demonstrate shape memory effect [7]. It is known that the amount of Al is more effective than that of Ni. Instead, improvement of the thermoelastic and pseudoelastic behavior of Cu–Al–Ni alloys by addition of a fourth and fifth element and the variation of the martensitic transformation temperatures with the addition of elements have been examined by number of researchers [8–16]. A survey on literature shows that there is no study on quaternary Cu–Al–Ni–Fe shape memory alloys. In this study, 4 mass%Fe was added into Cu–Al–Ni alloy and examined the effects of this addition on transformation temperature, crystal structure, microstructure, and microhardness by comparing the result to those obtained for traditional Cu–Al–Ni.

## Experimental procedure

Poly-crystal shape memory alloy with nominal composition of Cu–13%Al–4%Ni–4%Fe (in mass%) was prepared in an arc melting furnace with a water cooled Cu crucible

K. Yildiz (✉) · M. Kok  
Department of Physics, Firat University, 23119 Elazig, Turkey  
e-mail: kyildiz@firat.edu.tr

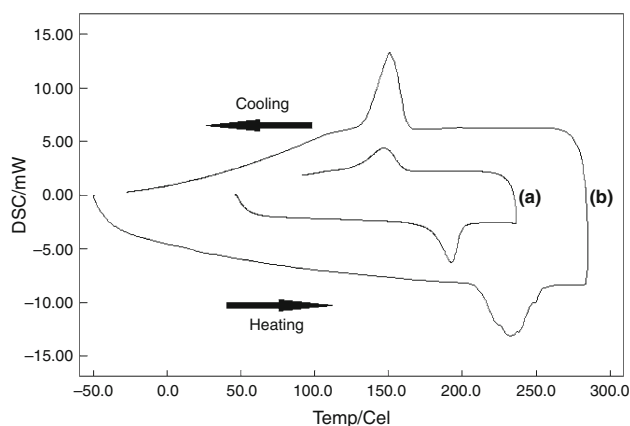


**Fig. 1** DSC curves of *a* as-homogenized and *b* heat-treated alloys

under vacuum using high purity elements Copper (99.8 %), Aluminum (99.9 %), Nickel (99.99 %), and Iron (99.9 %). The ingot was melted several times and then the alloy was annealed at 850 °C for 10 h for improved homogenization. The chemical composition of the alloy was determined to be 3.62 mass% O, 11.63 mass% Al, 3.24 mass% Fe, 3.43 mass% Ni, and 78.09 mass% Cu by using an energy dispersive X-ray spectrometry (EDX). As a result of homogenization at air atmosphere, the minor amount of oxygen was observed in EDX results. Some homogenized samples were heat treated at 950 °C during 1 h to eliminate strain effects which happen after cutting and homogenized alloys quenched in iced brine. The phase transformation temperature and the thermodynamic parameters were determined by Perkin Elmer Sapphire differential scanning calorimeter (DSC) at the heating-cooling rates of 25 °C min<sup>-1</sup> under an inert nitrogen atmosphere in the flow rate of 80 mL. TG/DTA measurement was done to investigate high temperature phase changes by Perkin Elmer Pyris TG/DTA device. In order to determine crystal structures of as-homogenized and heat-treated alloys, X-ray diffraction (XRD) measurements were carried out in the range of 20°–80° using Cu K $\alpha$  as the incident beam Bruker Discover D8 with the scanning rate of 2 min<sup>-1</sup>. The microstructures of alloys were characterized by NIKON optical microscopy. The samples, grinding with emery paper and then polishing, were etched by solution of 20 mL HCl, 5 g FeCl<sub>3</sub>–H<sub>2</sub>O, and 96 mL methanol. Vickers microhardness measurement was made using Emco Test DuraScan microhardness testing machine. Three measurements were carried out, on each alloy, and the average obtained.

## Results and discussion

Figure 1 shows the DSC curves of as-homogenized and the heat-treated Cu–Al–Ni–Fe alloys that were heated at a rate of 25 °C min<sup>-1</sup> under inert nitrogen atmosphere. Transformation

temperatures of both alloys, i.e.,  $A_s$  and  $M_s$  Austenite and martensite start temperatures;  $A_f$  and  $M_f$  austenite and martensite finish temperatures;  $A_p$  and  $M_p$  austenite and martensite maximum peak temperatures, are given in Table 1.

When the results given in Table 1 are examined, it can be seen that transformation temperature of the as-homogenized Cu–13%Al–4%Ni–4%Fe (in mass%) alloy is similar to the values given for Cu–Al–Ni alloys in the literature [17]. In general, the value of the transformation temperature of Cu–Al–Ni alloys lies between 100 and 200 °C [1, 17–19]. Here, it can be concluded that the addition of Fe does not have a significant effect on the transformation temperature of the alloy. It was observed that transformation temperature of the Cu–Al–Ni–Fe alloy increased when it was heat treated at 950 °C. Chen et al. [20] emphasized that there are two types of thermal transformation. In the first case, transformation occurs in the order of  $A_f > A_s > M_s > M_f$ , while in the second it occurs as  $A_f > M_s > A_s > M_f$ . According to this explanation, as-homogenized and heat-treated Cu–13%Al–4%Ni–4%Fe (in mass%) alloys demonstrate the second type of transformation.

By using the DSC data collected in the cooling and heating periods, the change in enthalpy values was determined for as-homogenized and heat-treated Cu–Al–Ni–Fe shape memory samples. A small variation in the enthalpy value occurred during cooling as a result of the acoustic emission [21]. In order to eliminate this difference, the average enthalpy value was calculated using the equation  $\Delta H_{ave} = (\Delta H_{heat} + \Delta H_{cool})/2$ . The change in the entropy value ( $\Delta S$ ) was calculated using the equation  $\Delta S = \Delta H_{ave}/T_0$  for which the calculated  $\Delta H_{ave}$  value was used [22]. Here, the value of  $T_0$  is the temperature at which the Gibbs free energy equals to zero and calculated by  $1/2(A_s + M_s)$ . On the other hand, Gibbs free energy in cooling is calculated as follows using the variation in enthalpy value in cooling and  $T_0$  equilibrium temperature:

$$\Delta G_v = \Delta H_{cool} \cdot \Delta T/T_0 \quad (1)$$

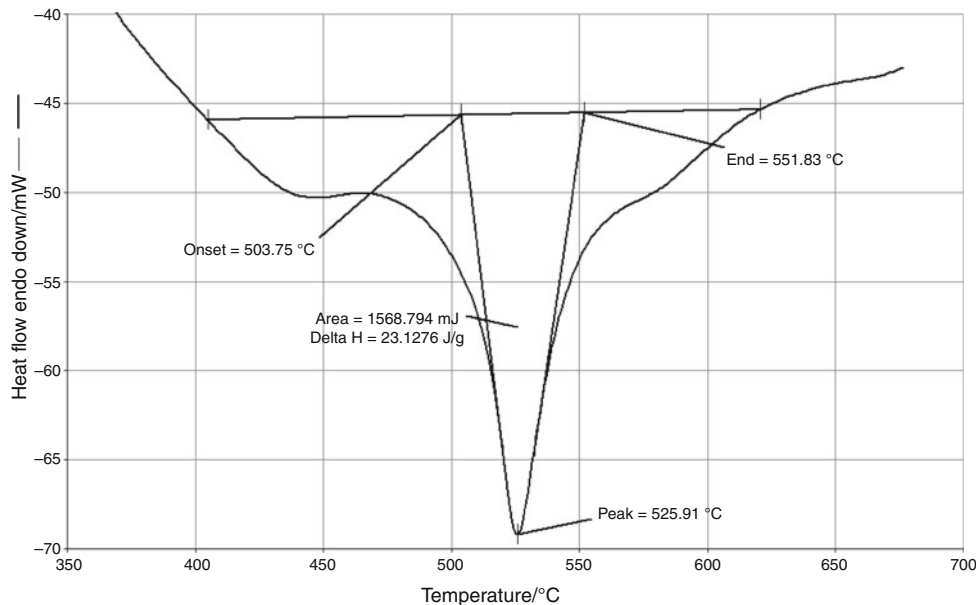
Here,  $\Delta T = T_0 - M_p$

For the alloy Cu–Al–Ni–Fe, an increase occurred in the average enthalpy change, entropy change, and Gibbs free energy change upon cooling [23].

In order to determine the high temperature transformation temperature of the Cu–13%Al–4%Ni–4%Fe (in mass%) shape memory alloy after arc melting, TG/DTA measurements were performed in open atmosphere by employing a heating rate of 20 °C min<sup>-1</sup>. DTA curve of the alloy for a range of 350–700 °C can be seen in Fig. 2. The salient feature of this graph is the presence of one small and one transformation curves. These two phase transformations are typical for Cu–Al-based alloys such that the first one is the transformation from irregular DO<sub>3</sub> structure to the B2 regular structure and the second one is

**Table 1** Transformation temperatures and thermodynamic parameters of alloys

Alloys	$A_s/^\circ\text{C}$	$A_p/^\circ\text{C}$	$A_f/^\circ\text{C}$	$M_s/^\circ\text{C}$	$M_p/^\circ\text{C}$	$M_f/^\circ\text{C}$	$T_o/^\circ\text{C}$	$\Delta H_{ave}/\text{J g}^{-1}$	$\Delta S/\text{J g}^{-1} \text{ }^\circ\text{C}^{-1}$	$\Delta G_v/\text{J g}^{-1}$
As-homogenized	178.8	192.5	200.3	160.8	147.3	129.6	169.8	8.47	0.050	-1.01
Heat-treated	209.3	232.5	250.4	162.5	151.1	133.0	185.9	9.76	0.052	-1.63

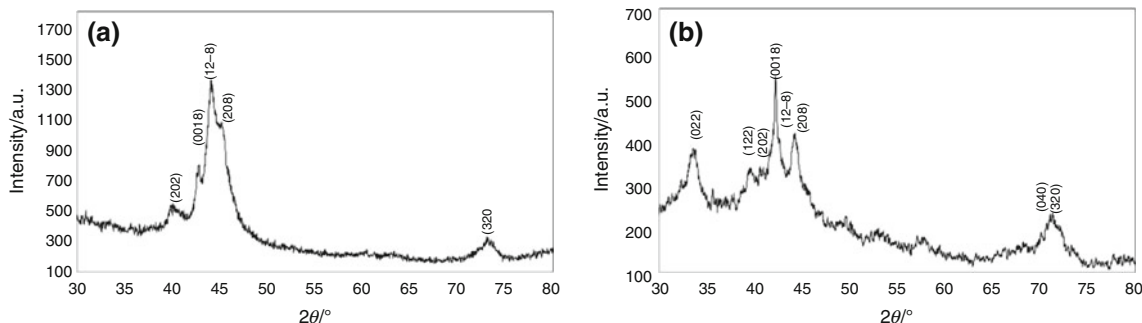
**Fig. 2** DTA curve obtained for as-homogenized alloy in the range of 350–700 °C

the transformation from regular B2 structure to irregular A2 structure [24, 25].

XRD pattern of the as-homogenized alloy sample is shown in Fig. 3a. As seen from the figure, in the pattern of the as-homogenized sample, some peaks overlap with each other forming a broad peak where splitting occurs. These splits are critical for Cu-based shape memory alloys and can be used in the qualitative analysis of the regularity in the martensite phase [26–28]. In this study, it is considered that this broad peak has such a splitted appearance as a result of the shear stresses developed during cutting of the sample. For this reason, heat treatment was applied at 950 °C for 1 h so as to remove the additional stresses

originating from the cutting process and after that XRD measurement was obtained. XRD pattern of the heat-treated alloy sample is shown in Fig. 3b. As a result of the applied heat treatment, broad peak disappeared and some peaks sharpened. On the other hand, both as-quenched and heat-treated alloy samples have maximum diffraction peaks in their diffraction patterns shown in Fig. 3a, b. The presence of these maximum diffraction peaks demonstrates that the alloy has M18R structure in both conditions. Indexed peaks are shown in Fig. 3a, b.

When X-ray diffraction patterns shown in Fig. 3a, b are evaluated simultaneously, it can be seen that position and strength of some peaks vary. Especially, peaks belonging

**Fig. 3** The XRD patterns taken from: **a** as-homogenized and **b** heat-treated alloys

to (040) and (320) shown in Fig. 3b started to overlap with each other. Miller indices of this pair of plane satisfy the special equation given below [29, 30]:

$$\frac{h_1^2 - h_2^2}{3} = \frac{k_2^2 - k_1^2}{n}.$$

For that reason,  $n$  is equal to 4 for the martensite 18R structure and the corresponding pairs of plane can be listed as follows: 12-2—202, 12-8—208, 1210—20-10, and 040—320. This observation can be based on a relation between interplanar spacing of these pairs of planes [30].

Crystal sizes of as-homogenized and heat-treated alloy samples ( $D$ ) were calculated by employing full width half maximum (FWHM) values of the strongest peak of the X-ray diffraction patterns shown in Fig. 3a, b into Scherrer equation [31]. The values were calculated as  $\sim 14.62$  and  $25.65$  nm for as-homogenized and heat-treated alloy sample, respectively. As expected and can be seen from calculated  $D$  values, the heat treatment increased the crystal size of the alloy.

Micro-strain ( $\varepsilon$ ) values of the as-homogenized and heat-treated samples were calculated using Williamson–Hall equation [32]. For as-homogenized and heat-treated samples, the values were calculated as  $\sim 2.819 \times 10^{-3}$

and  $\sim 1.668 \times 10^{-3}$ , respectively. These results showed that heat treatment yields a 60 % release in the strain, which are in good agreement with the X-ray diffraction patterns of the peaks shown in Fig. 3a, b. As a result of the release in strain, overlapped broad peaks separated from each other.

Optical micrographs of as-homogenized and the heat-treated Cu–13%Al–4%Ni–4%Fe (in mass%) shape memory alloy are demonstrated in the Fig. 4. In Fig. 4a, b, micrographs of the as-homogenized alloy at two different magnifications are shown. In Fig. 4a, grains can be clearly seen. Martensite lamellar structure can be observed in light and dark grains shown in Fig. 4b. In Fig. 4b, while parallel martensite plates are seen in the left grain, in the right one coarser martensite plates are drawing attention. Another remarkable point is the presence of the precipitates (Inset in Fig. 4b). These precipitates are different from what is observed in the microstructure of Cu–Al–Ni alloys [33]. The reason of precipitate formation could be presence of Fe.

In Fig. 4c, d, optical micrographs of the Cu–13%Al–4%Ni–4%Fe (in mass%) alloy at different magnifications are given for the sample heat treated at 950 °C for 1 h. The images show that the heat-treated sample has quite

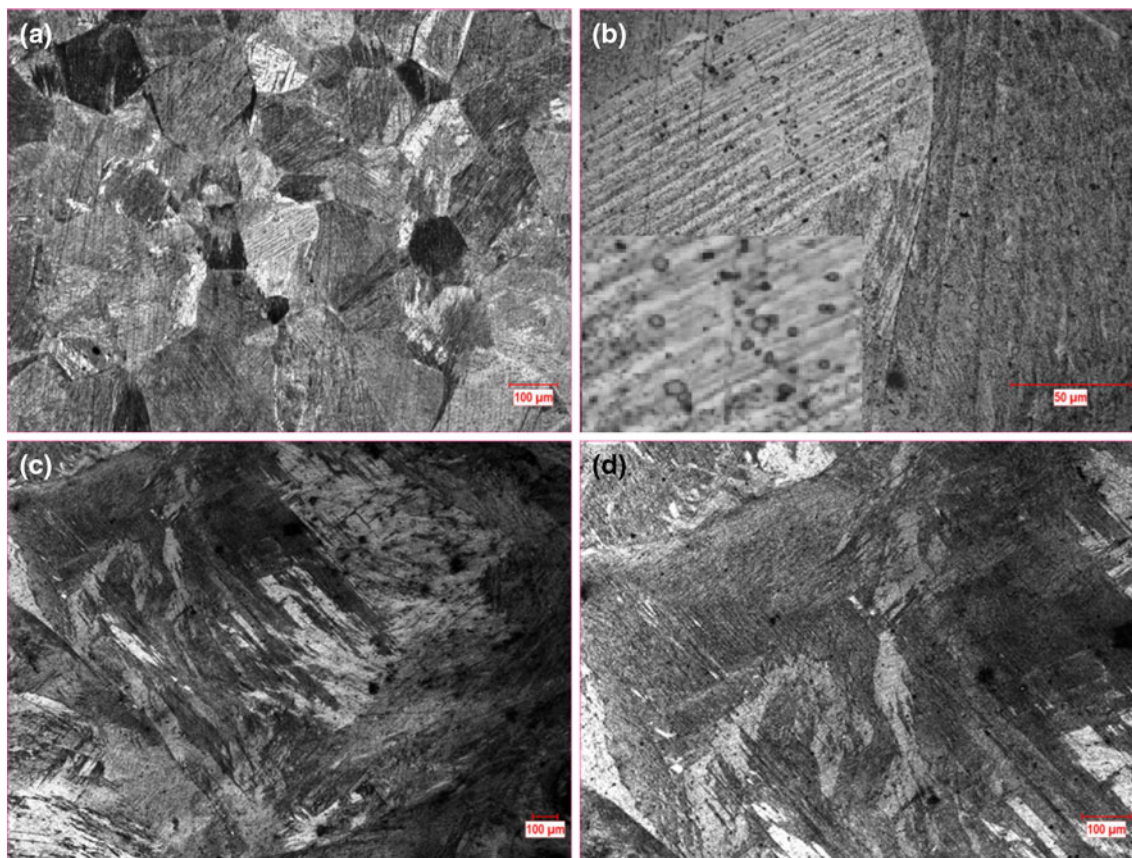


**Fig. 4** Optical micrographs taken from **a, b** as-homogenized and **c, d** heat-treated alloys

**Table 2** Vickers microhardness values of alloys

Samples	1/Hv	2/Hv	3/Hv	4/Hv	5/Hv	Average/Hv
As-homogenized	363	365	363	356	360	361
Heat-treated	394	394	358	367	363	375

different microstructures than homogenized one. Coarse martensite plates were observed in the microstructure. In Fig. 4d, V-type martensite plates can be seen.

Five consecutive Vickers microhardness measurements were taken from as-homogenized and the heat-treated Cu–13%Al–4%Ni–4%Fe (in mass%) shape memory alloys and average of them was taken as the Vickers microhardness value. In both alloys, hardness value was different at each measurement, while it was taken from the same surface. This was the result of the fact that the indentation point was at different grains in each measurement (Table 2). It was observed that the microhardness value increases with heat treatment. In the study performed by Aydoğdu, the hardness value of the Cu–Al–Ni alloy was found as 281 Hv for as-homogenized sample and found as 321 Hv when heat treatment was performed at 930 °C [34]. Hardness value measured for Cu–13%Al–4%Ni–4%Fe (in mass%) alloy was 361 and 375 Hv for as-homogenized and heat-treated samples, respectively. Both of these values are higher than those given for Cu–Al–Ni alloys in the literature. According to Gojic et al. [35] study, the microhardness value of Cu–13.16%Al–4.11%Ni shape memory alloys was found as 275 Hv. Other study, Rezvani and Shokuhfar [36] produced two different percentages of Cu–Al–Mn shape memory alloys and they found microhardness values of these alloys about 220 Hv. It can be considered that the reason of this increase is the addition of Fe.

## Conclusions

The examination of the polycrystalline Cu–13%Al–4%Ni–4%Fe (in mass%) shape memory alloy produced by arc melting technique showed the following results:

- DSC and DTA experiments showed that the addition of Fe did not make a significant difference in the transformation temperatures and phase structure.
- Optical microscope images showed that in both conditions crystallized grain structure with parallel martensite plates. On the other hand, the thickness of the martensite plates increased with heat treatment performed at 950 °C.
- XRD results showed that the martensite alloy had 18R crystal structure. By the effect of heat treatment, it was observed that while the crystallite size was increased, the micro-strain was relaxed.

- Significant number of randomly distributed Fe precipitates was detected in the as-homogenized alloy. These precipitates dissolved in the matrix when 950 °C heat treatment was conducted.
- Increase in the Vickers hardness of the as-homogenized alloy with the addition of Fe was higher than that was reported in the literature. This difference becomes more apparent upon heat treatment.

## References

1. Recarte V, Perez-Landazabal JI, Ibarra A, No ML, Juan JS. High temperature  $\beta$  phase decomposition process in a Cu–Al–Ni shape memory alloy. *Mater Sci Eng A*. 2004;378:2–238.
2. Recarte V, Perez-Landazabal JI, Rodriguez PP, Bocanegra EH, No ML, Juan JS. Thermodynamics of thermally induced martensitic transformations in Cu–Al–Ni shape memory alloys. *Acta Mater*. 2004;52:3941–8.
3. Sari U, Kırındı T. Effects of deformation on microstructure and mechanical properties of a Cu–Al–Ni shape memory alloy. *Mater Charact*. 2008;59:920–9.
4. Chung CY, Lam CWH. Cu-based shape memory alloys with enhanced thermal stability and mechanical properties. *Mater Sci Eng A*. 1999;273–275:622–4.
5. Sari U, Aksoy I. Micro-structural analysis of self-accommodating martensites in Cu–11.92 wt% Al–3.78 wt% Ni shape memory alloy. *J Mater Process Technol*. 2008;195:72–6.
6. Delaey L. Diffusionless transformations. In: Haasen P, editor. *Phase transformation in materials*. Weinheim: VCH; 1991.
7. Otsuka K, Wayman CM. *Shape memory materials*. Cambridge: Cambridge University Press; 1998.
8. Sugimoto K, Kamei K, Mtsumoto H, Komatsu S, Akamatsu K, Sugimoto T. Grain-refinement and the related phenomena in quaternary Cu–Al–Ni–Ti shape memory alloys. *J de Physique Colloque*. 1982;C4:761–6.
9. Lee JS, Wayman CM. Grain refinement of a Cu–Al–Ni shape memory alloy by Ti and Zr additions. *Trans Jpn Inst Met*. 1986;27:584–91.
10. Morris MA, Lipe T. Microstructural influence of Mn additions on thermoelastic and pseudoelastic properties of Cu–Al–Ni alloys. *Acta Metall*. 1994;42:1583–94.
11. Morawiec H, Lelatkó J, Stroz D, Gigla M. Structure and properties of melt-spun Cu–Al–Ni shape memory alloys. *Mater Sci Eng A*. 1999;273–275:708–12.
12. Dutkiewicz J, Czepe T, Morgiel J. Effect of titanium on structure and martensic transformation in rapidly solidified Cu–Al–Ni–Mn–Ti alloys. *Mater Sci Eng A*. 1999;273–275:703–7.
13. Segui C, Pons J, Cesari E, Muntasell J, Font J. Characterization of a hot-rolled Cu–Al–Ni–Ti shape memory alloy. *Mater Sci Eng A*. 1999;273–275:625–9.
14. Xiao Z, Li Z, Fang M, Xiong S, Sheng X, Zhou M. Effect of processing of mechanical alloying and powder metallurgy on microstructure and properties of Cu–Al–Ni–Mn alloy. *Mater Sci Eng A*. 2008;488:266–72.
15. Stanciu S, Bujoreanu L-G, Özkal B, Öveçoğlu ML, Sandu AV. Study of precipitate formation in Cu–Al–Ni–Mn–Fe shape memory alloys. *J Optoelectron Adv Mater*. 2008;10:1365–9.
16. Goryczka T. Effect of wheel velocity on texture formation and shape memory in Cu–Al–Ni based melt-spun ribbons. *Arch Metall Mater*. 2009;54:755–63.
17. Zengin R, Ceylan M. Influence of neutron irradiation on the characteristic of Cu–13% wt. Al–4% wt. Ni shape memory alloy. *Mat Lett*. 2003;58:55–9.

18. Suresh N, Ramamurty U. Aging response and its effect on the functional properties of Cu–Al–Ni shape memory alloys. *J Alloy Compd.* 2008;449:113–8.
19. Bouabdallah M, Baguenane-Benalia G, Saadi A, Cheniti H, Gachon JC, Patoor E. Precipitation sequence during ageing in  $\beta_1$  phase of Cu–Al–Ni shape memory alloy. *J Therm Anal Calorim.* 2013;112:279–83.
20. Chen F, Wang HB, Zheng YF, Cai W, Zhao LC. Effect of Fe addition on transformation temperatures and hardness of NiMnGa magnetic shape memory alloys. *J Mater Sci.* 2005;40:219–21.
21. Kok M, Aydogdu Y. Effect of heat treatment on the physical properties Ni–Mn–Ga alloy. *Thermochim Acta.* 2012;548:51–5.
22. Kok M, Yakinci ZD, Aydogdu A, Aydogdu Y. Thermal and magnetic properties of Ni<sub>51</sub>Mn<sub>28.5</sub>Ga<sub>19.5</sub>B magnetic shape memory alloy. *J Therm Anal Calorim.* doi:10.1007/s10973-013-3365-z.
23. Kok M, Aydogdu Y. Effect of composition on the thermal behavior of NiMnGa alloys. *J Therm Anal Calorim.* 2013;113: 859–63.
24. Stanciu S, Bujoreanu LG, Ionita I, Sandu AV, Enache A. A structural-morphology study of a Cu<sub>63</sub>Al<sub>26</sub>Mn<sub>11</sub> shape memory alloy. *Proc SPIE.* 2009;7297:72970C1–4.
25. Lazzini F, Romero R, Castro ML. Influence of Be addition on order–disorder transformation in  $\beta$  Cu–Al. *Intermetallics.* 2008;16:1090–4.
26. Adiguzel O, Chandrasekaran L, Miodownik AP. The role of ordering in the loss of shape memory in some copper-base alloys, the martensitic transformation in science and technology. In: Hornbogen E, Jost N, editors. *Informationsgesellschaft.* Bochum: Verlag; 1989. p. 109–14.
27. Xuan Q, Bohong J, Hsu TY. The effect of martensite ordering on shape memory effect in a copper–zinc–aluminium alloy. *Mater Sci Eng A.* 1987;93:205–11.
28. Aydogdu A, Aydogdu Y, Adiguzel O. The influence of ageing on martensite ordering and stabilization in shape memory Cu–Al–Ni alloys. *Mater Res Bull.* 1997;32:507–13.
29. Kayali N. CuZnAl Alaşımalarında Martensit Stabilizasyonu ve Taşlama Etkileri. Ph.D. Thesis, Firat University, Elazig, Turkey; 1993 (in Turkish).
30. Aydogdu A, Aydogdu Y, Adiguzel O. Long-term ageing behaviour of martensite in shape memory Cu–Al–Ni alloys. *J Mater Process Technol.* 2004;153–154:164–9.
31. Cullity BD. *Elements of X-Ray diffraction.* Massachusetts: Addison-Wesley Publishing Company; 1978.
32. Williamson GK, Hall WH. X-ray line broadening from filed aluminium and wolfram. *Acta Metall.* 1953;1:22–31.
33. Izadinia M, Dehghani K. Structure and properties of nanostructured Cu-13.2 Al-5.1 Ni shape memory alloy produced by melt spinning. *Trans Nonferrous Met Soc China.* 2011;21:2037–43.
34. Aydogdu A. Thermal ageing effects on martensitic transformation in shape memory CuAlNi alloys. Ph.D. Thesis, Firat University, Elazig, Turkey; 1995.
35. Gojic M, Kozuh S, Anzel I, Lojen G, Ivanic I, Kosec B. Microstructural and phase analysis of CuAlNi shape memory alloy after continuous casting. *MTAEC9.* 2013;47–2:149–52.
36. Rezvani MR, Shokuhfar A. The effect of chemical composition on crystal size and mechanical properties of nanostructured Cu–Al–Mn shape memory alloy prepared by mechanical alloying technique. In: *Proceeding of 4th International conference on nanostructure (ICNS4);* 2012:1525–1527.